A Study of Reflector-Enhanced Bifacial PV

Matthew Rueter, Mariam Dobosz, Richard D. Wilk
Mechanical Engineering Department
Union College, Schenectady, NY

Abstract

Bifacial solar PV is a promising technology that can increase the amount of power generated by harvesting power on both sides of a module. Understanding how best to configure the geometry of these bifacial solar collectors is non-trivial as many geometric factors (tilt, ground reflectance (albedo), height above ground, row spacing, module spacing) tend to be interdependent, requiring a case by case analysis in order to optimize the total power output and maintain the frontside incident irradiance while maximizing the backside gain. In addition, as with monofacial modules, use of planar reflectors can be a cost effective way of increasing the incident irradiance, in the case of bifacial modules, on both sides of the module. However, the addition of reflectors adds to the challenge of optimizing the system configuration. The work described here presents an experimental and modeling study of reflector enhanced bifacial modules. Experiments were conducted on bifacial modules with and without reflector augmentation and compared against monofacial PV modules, assessing the effects of specular and diffuse reflectors. A model was developed to calculate the incident and reflected irradiance on the front and back sides of the modules. Beam insolation components were handled with ray tracing and sky and reflected diffuse components were handled with view factors.

Keywords: Bifacial PV, Bifacial Irradiance Model, Reflectors

---

1. Introduction

Bifacial solar is a promising technology in solar PV with the potential to further reduce the levelized cost of electricity. The concept of collecting and converting sunlight from both sides of a solar collector has been studied for nearly 60 years, including the investigation of solar PV and solar thermal collectors (often referred to as double-exposure collectors). Bifacial solar PV modules are the focus of this study. The transparent back sheet of bifacial PV modules allows them to collect light on the rear surface as well. This increases the power generation of the module per unit area as compared to the traditional monofacial counterpart. This could allow for smaller arrays that occupy less land area while producing the same power and potentially reduce some balance of plant costs. A review of the state of the technology was done by Guerrero-Lemus, et al. (2016).

Various studies of bifacial cells and modules through the years have demonstrated the production of up to about 50% additional energy (Cuevas et al. (1982)) under idealized conditions, but more typically 10-30% under more realistic conditions (Sun et al. (2018)). In the field, getting the most out of a bifacial module requires optimizing the configuration in a way that will maximize the annual energy output. Variables affecting this include the module tilt angle, the surface azimuth angle, the height of the module above the ground, the

doi:10.18086/solar.2021.01.05 Available at http://proceedings.ises.org

reflectance of the ground (albedo) and the spacing between successive rows in the array. The big challenge with bifacial is to maximize the irradiance striking the back side, while maintaining a high level of irradiance to the front side, which is the primary power generating part of the module. The bifacial gain factor BG is used as an indicator of this relationship and is the ratio of the back side power to the frontside power. Many studies, for example Yusufoglu et al. (2014), have studied the effects of these variables on the backside irradiance and on BG. Coming out of this body of work it was clear that there are interdependencies of some of these variables and that nonuniformity of light reaching the backside is an important issue (Kreinin et al. (2010); Yusufoglu, et al. (2015)).

Computational modeling can be applied to cut down on the needed time and expense of optimizing mounting arrangements. However, some experimental data is still required to validate the functionality and performance of the models. Mostly over the last 15 years, predictive models have been developed to accurately predict the rear surface incidence to aid in the system design and to optimize the system configuration. These have been compared with each other and validated with available system data (Pelaez et al. (2019)). To model the rear side irradiance, models use either view factors, ray tracing, a combination of both or simpler geometric relationships (Hansen et al. (2016); Jäger et al. (2020); (Durusoy et al. (2020)). View factors are parameters that indicate what fraction of light is reflected onto a surface from nearby surfaces and are computationally less demanding, while ray tracing simulates and follows the directional paths light travels and tends to be better at capturing the non-uniformity.

Although many mountings of bifacial panels are similar to ones for monofacials, some different and novel arrangements have been proposed and analyzed (Joge et al. (2002); Karahara et al. (2003); Guo et al. (2013); Appelbaum (2016); Khan et al. (2017); Sun et al. (2018)) like vertical tilt and east-west facing modules to alter the daily and seasonal power production profile and to fit more collectors into an array.

For a number of years, concentrators and various reflectors have been proposed as a cost-effective way of enhancing the incident irradiance to a collector surface and hence, increasing the power output. This has been the subject of many studies related to thermal collectors and monofacial PV. This concept has also been applied to bifacial modules (Moehlecke et al. (2013); Ooshaksaraei et al. (2013); Jakobsen et al. (2019)). As the bifacial gain is proportional to the amount of light that is reflected onto the back of the panel, the use of reflectors has been investigated as a way to increase the power gain. In this case, additional variables become important like the collector-reflector spacing, height, tilt, size and reflectance of the reflector. With no reflector present, the ground reflected and sky diffuse sunlight behind the collector are normally key in bifacial applications as they are the primary mechanisms by which the rear side of the collector gets irradiated. Therefore, the presence of a reflector would have to complement and not interfere significantly with these other sources. Many possible reflector designs have been proposed, simple ones including mirrors and while paint More complicated reflectors include the use of light scattering beads or powders, adjustable mirror arrays, and prisms (Lim et al. (2014)).

In this work, a model was developed to determine the front and back incident irradiance on a bifacial solar collector equipped with a rear planar reflector. The model calculates hourly incident irradiance on the front and back sides of a module in most any location for different geometric arrangements. Reflectors can be added to the setup as well and their effect on the incident energy can be calculated as well as potential shading interference. In addition, experiments were set-up and run with surrogate bifacial modules to study some of these variables, and to assess the effects on the rear incident energy of the addition of planar reflective surfaces behind the collector. In addition, the experimental results were compared with the modeling results, to demonstrate the model's ability to predict potential shading interference and to calculate the incident radiant energy striking the front and back sides of a module equipped with a rear reflector. This paper presents some preliminary results from the experiments and modeling cases.

2. The Model

A model for simulating incident energy on solar panels was developed and programmed in the Python coding language. The model used the Numpy and Matplotlib modules in Python. In general, the model is designed to be modular and functions have been written to perform basic calculations. It is intended that this model will serve as an informative collection of functions that can be rearranged for various purposes. The code has the ability to track the sun across the sky, calculate the incident energy on a surface, and model shading and reflected light with ray tracing and view factors.

Tracking the position of the sun was accomplished by calculating the solar altitude angle and solar azimuth angles (Duffie and Beckman (2013)). Solar insolation data was obtained from the National Solar Radiation Database (NSRDB). Hourly data for beam, diffuse, and total insolation on the horizontal surface were obtained and processed to produce average values for hourly insolation in a typical day of each month of the year (monthly average hourly insolation). For a given hour of the day in a given month, the recorded insolation in that hour for every day of the month was averaged, producing a single value for that hour. Functionality was also included to calculate monthly average daily insolation, which was done by summing the total insolation over a month and dividing it by the number of days in the month. Once the insolation data has been processed as desired for one year, the results can be averaged with other years to produce multi-year averages.

The insolation on a tilted surface in a given hour assumes the isotropic sky diffuse model and involves beam, diffuse and ground reflected and is calculated with

$$I_T = (I - I_d)\frac{\cos(\theta)}{\cos(\theta_z)} + I_d\frac{1+\cos(\beta)}{2} + I\rho\frac{1-\cos(\beta)}{2} \quad \text{(eq.1)}$$

where I_T is hourly insolation on the tilted surface, I is the total hourly insolation on the horizontal, I_d is the hourly diffuse insolation on the horizontal, θ is the incidence angle calculated at the middle of the hour being studied, θ_z is the zenith angle in the middle of the hour, and ρ is the ground reflectance (Duffie and Beckman, 2013).

To move from insolation per square meter to insolation on a surface, the surfaces of collectors and reflectors modeled were described using a grid. The grid breaks the surface into small 2-D square cells that are treated as having the same amount of light shining over their entire surface. In this way the distribution of solar energy across the surface can be broken into discrete elements instead of being modeled as a continuum. A single

parameter defines the side length and grid sizes can be changed by changing this length, allowing coarser or finer grids to be used.

Ray tracing methods were applied to study the effects of reflectors and shading between rows. Rays are assumed to move in a straight line from the sun's location. A specular reflector like a mirror will reflect light from it at an angle equal to the incidence angle and in the same plane normal to the surface at which it struck the panel. This allows reflection to be modeled. Where a collector surface intercepts these rays an extra beam term is added to a list. The total energy of a reflected beam of light is calculated based on the area of the grid element it reflects from on the reflector. All irradiance terms coming from the reflector are multiplied by the collector reflectance, allowing for the modeling of non-ideal reflectors. For shading, the model traces rays of light intercepted by a front row panel back as if the panel was not there to see where they strike the rear panel or reflector. Any parts of a rear row panel or reflector that has its incident rays blocked by the module are considered shaded and no beam irradiance reaches them.

For sky diffuse and reflected diffuse from the ground and reflector, radiation view factors are used. In this work we studied the case of a reflector behind a bifacial collector where both are vertical and aligned (Fig. 1).

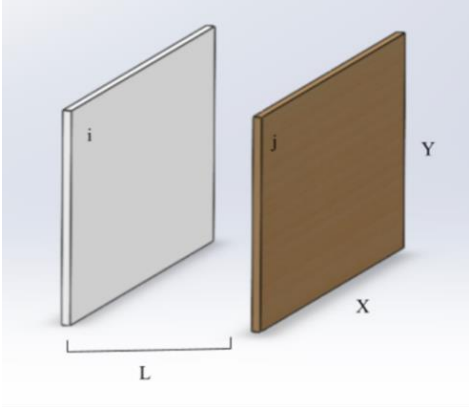

Fig. 1: Geometry for parallel surface view factor where i is the reflector and j is the collector.

In this case a 3-D view factor between the aligned vertical plates is used (Bergman, et al. (2011)).

$$F_{ij} = \frac{\mathbf{2}}{\boldsymbol{\pi xy}}\left[ln\left(\frac{(1+\bar{x}^2)(1+\bar{y}^2)}{1+\bar{x}^2+\bar{y}^2}\right)^{1/2} + \bar{x}\left(y_1 arctan\frac{\bar{x}}{y_1}\right) + \bar{y}\left(x_1 arctan\frac{\bar{y}}{x_1}\right) - (\bar{x})arctan(\bar{x}) - (\bar{y})arctan(\bar{y})\right] \quad \text{(eq. 2)}$$

where:

$\bar{x} = \frac{x}{L}$ $\quad \bar{y} = \frac{y}{L}$ $\quad x_1 = \sqrt{1+\bar{x}^2}$ $\quad y_1 = \sqrt{1+\bar{y}^2}$

The focus of this study was on the effects of the reflectors, so it was desired to try to isolate this aspect and remove from the computation the effect of ground albedo, which is a contributor to both the front and especially the back side irradiance. Therefore, the ground reflected subroutine was not used in the modeling. In order to match this in the experiments (discussed below) black matte roofing paper was placed all around the collector

and reflector to try to reduce the ground reflected component as much as possible to isolate the irradiance from the reflector and the sky.

3. Experiments

Three separate experimental systems were used to generate experimental data related to bifacial collectors equipped with rear reflectors. The purpose was to understand how some of the key factors that affect the amount of irradiance striking both sides of the collectors and to help validate the model that was developed. The first used simple parallel planar surfaces facing south that were used to validate the accuracy of the shading calculations of the model. This was done by taking photos of the shading patterns on the rear surface (representing the reflector) at different times. The second involved a south-facing collector-reflector pair with the reflector frame set up behind the collector. A bifacial collector was represented in this experiment by a planar panel with the rear side outfitted with six PV cells. These cells were calibrated and used as sensors to measure the irradiance striking the rear side (Fig. 2 a and b) from rear side sources like the sky, ground and rear side reflector. Each of the sensor cells was configured with a 2 ohm resistor and the voltage across the resistor was measured and calibrated over a full range of solar insolation against a Kipp and Zonen Pyranometer.

Fig: 2: a) 3D rendering of the orientation for the second experimental setup and image of b) photovoltaic cells simulating different positions on the rear side of a collector

This set-up allows for the changing of the collector and reflector size and spacing between them, the height from the ground of the collector and reflector, the collector tilt, and azimuth. The cells were placed on the back side of the module used to measure the back side irradiance. The pyranometer was used to measure the front side irradiance and together they were used to determine a measured bifacial gain (BG) factor in terms of a ratio of the back to front irradiances for the given geometric configuration. The rear side reflectance was achieved by placing a reflective surface behind the collector. For this study the reflectors were aligned and parallel to the front panel and they had the same width and height. The set-up allowed the reflectors to be easily changed out in a short time. Two different reflector surfaces were used, reflective Mylar sheet on a substrate and a white diffuse FRP panel. The pyranometer voltage output and the voltages across the calibrated cells were measured and logged using a Measurement Computing data acquisition system.

In the third system, single crystal 50 W monofacial PV modules were placed back-to-back and used to represent bifacial modules. The advantage to this versus using actual bifacial modules is that the power output on the front and back can be measured individually to determine the bifacial gain as a function of a number of

geometric and reflector parameters. Both set ups with the back-to-back monofacial modules were held up by metal frames with reflectors of the same size behind them. Each set-up had a different reflector or no reflector, to compare the effects of different reflectors under the same sun conditions. A third frame with a single monofacial module of the same spec was used to provide a monofacial baseline power output (Fig. 3). Since we were using five of the same monofacial modules in this set-up, we had to ensure that all five modules yielded the same power output. To do this all five modules used were run side by side for several days.

Fig. 3: Experimental Set-Up Using Back-to-Back Monofacial PV Modules

4. Results

To begin, tests were performed to validate the model's capabilities. Figure 4 shows a rendering of how the code previews the correct geometry in three dimensions and demonstrates shading or reflection that occurs during the simulation. The parameters associated with the collector (right surface) and reflector (left surface) geometry, like tilt and surface azimuth angles, height of the modules above the ground, spacing between reflector and collector will be indicated, along with any shading of either surface by the other, and reflected illumination.

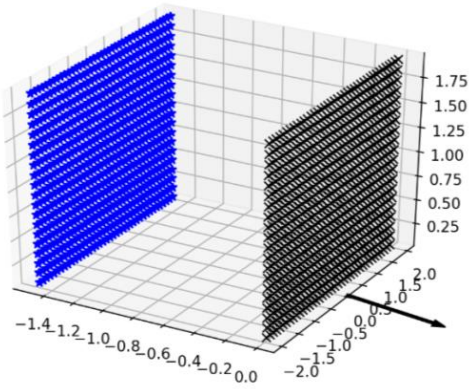

Fig. 4: Geometry for demonstrations of combined shading, reflection, and irradiance analysis. Each of the collector (right) grid points are marked with an X and stars mark the grid points of the reflector (left). The arrow to the right points south.

An experimental verification of the shading model was carried out using a panel representing a collector 0.6096 m high by 1.219 m wide, mounted with a tilt of 45° with a surface azimuth angle of 0°. A reflector of the same

size and tilt was mounted 1.219 m behind the collector. Both the collector and reflector used grid spacings of 0.1 m. The location used was Plymouth Meeting, PA (ϕ=40.14°) for the date of December 15. A comparison of the experimental and modeled shading achieved in the multi-row shading test is shown in Fig. 5a and b. In general, the agreement between the experimental and simulated results is fairly close, showing that the measured shading
matches the calculated shading for this geometry.

Figure 6 shows experimental and modeling results over a day for a collector-reflector system in Schenectady, NY (ϕ=42.8°) on July 5. The experimental results are from the rooftop system with calibrated cell sensors on the rear of the surrogate bifacial module, measuring the rear irradiance (Fig. 2 a and b). A Kipp and Zonen pyranometer is vertically mounted to the collector and measures the front side irradiance. Bifacial gains are determined from the ratio of the rear and front measured irradiances. For this case a diffuse white FRP panel was used as the rear reflector (reflectance=0.78), mounted 1 m behind and parallel to the collector. Both surfaces were 1.219 m wide and 0.6096 m high, oriented vertically, facing due south and raised 1 m off the ground. As mentioned earlier, black, light absorbing roofing paper was placed horizontally in front of both the collector and the reflector and vertically in the 1 m space below the reflector to greatly reduce any ground reflected irradiance to the rear side of the collector. Data was collected beginning at about 10 am standard time and continued to sunset. Bifacial gains reached 0.37$\pm$0.03 in the four hours centered around noon and trended higher as sunset approached, exceeding 1.0 which is consistent with the crossover of the sun back into the northern sky at this time of year, at which point the rear of the module sees direct solar irradiance. This effect is shown in the modeling results on Fig. 6, as well. The calculated BG values from the model spike in the morning and afternoon, but maintain a BG average of 0.38$\pm$0.03 around midday, in good agreement with the experiments.

Figure 7 shows the model irradiance results for this case, with the individual components of the front and rear sides plotted over the day. Ground reflected on either side of the collector was not included. The rear side

components (beam and diffuse) each include both incident sky and reflected terms. The rear beam and total show a similar shape to the BG plotted in Fig 6. However, the beam components on the rear side drop to zero during the middle of the day for this case. This is due to the 1 m spacing between the reflector and collector and the large incidence angle of the sun on a vertical surface during the day at this time of year. Any beam reflected from the reflector does not strike the back of the collector.

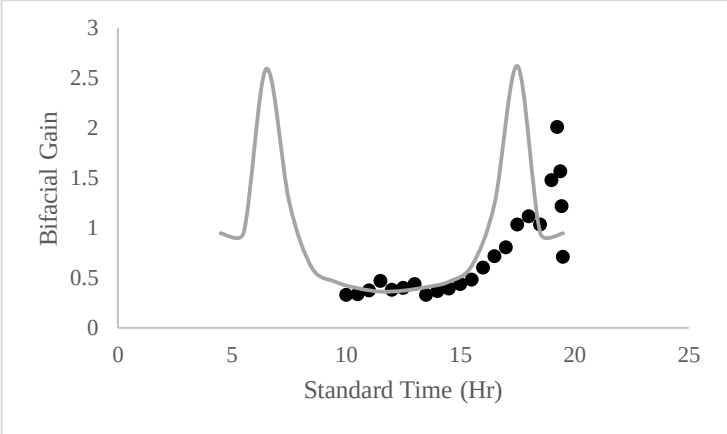

Fig. 6: Overlay of experimental (points) and model predictions (smooth line) for a vertical configuration of collector with a diffuse reflector on July 5, 2021.

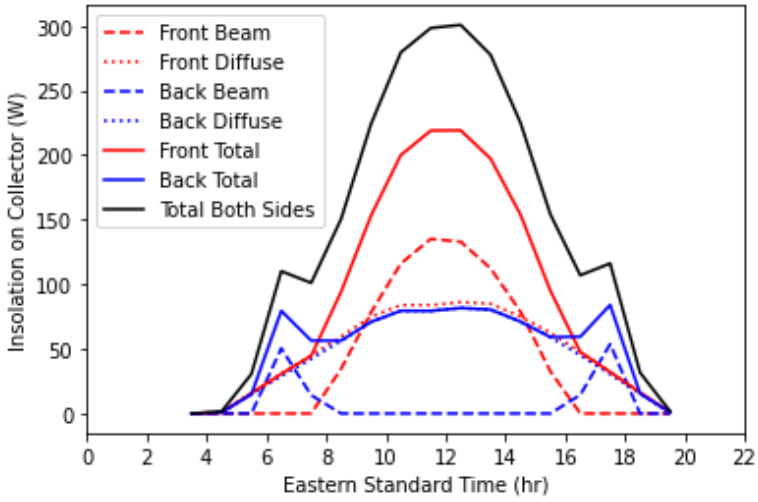

Fig 7: Model output of each sunlight component for a vertical collector and white diffuse collector on July 5, 2021.

For the case shown in Fig. 8, the set-up was maintained and run on a different day where the white diffuse reflector was replaced with a Mylar film reflector (reflectance 0.82). In these experiments, the data is started early in the day to capture the activity near sunrise and during the solar crossover into the southern sky. The model does a decent job at capturing this crossover and the mid-day BG values. There is more scatter in the experimental data on this day due to the variability in the sunlight. The mid-day (10am-2pm) experimental and modeling BG values for this case are 0.64 and 0.43 respectively.

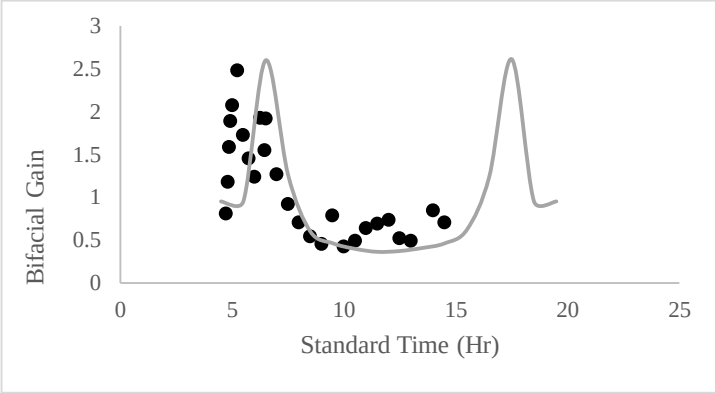

Fig. 8: Overlay of experimental (points) and model prediction (smooth line) for a vertical configuration of a collector and Mylar reflector on July 5, 2021.

Figures 9 and 10 show experimental results from the other roof-top experiment that used twin back-to-back monofacial single crystal 50 W PV modules, along with a single monofacial module for comparison, all under the same sunlight. Each back-to-back system had the option for a rear reflector. For all of the cases described here the collectors and reflectors were south-facing vertical and parallel. The collectors and reflectors were 0.6858 m wide by 0.5334 m high raised up 0.9525 m from the ground and the reflector-collector spacing was 0.5334 m. A calibrated cell, like the ones used in the other experiment, was used here on the front to measure the insolation striking a vertical south-facing surface. As with the other experiment, black absorbing roofing paper was placed all around the set-up to reduce the ground reflected component. In the case of Fig. 9, no reflector was used in the first system and the second system used a white diffuse reflector. The power output was measured from each of the front and rear modules over the central part of a day which allowed the calculation of the BG values shown in Fig. 9. The BG for the no reflector case results just from the rear sky diffuse averaging about 0.16 over the hours tested. The white diffuse reflector showed much better output, averaging a BG of about 0.22, or 35% higher than the no-reflector case. During the hours tested, there was no direct or reflected beam components on the rear side due to the collector-reflector spacing and the high altitude angle of the sun. The front insolation is also plotted on the figure. The BG values tend to rise when the insolation is low and fall when the insolation is high.

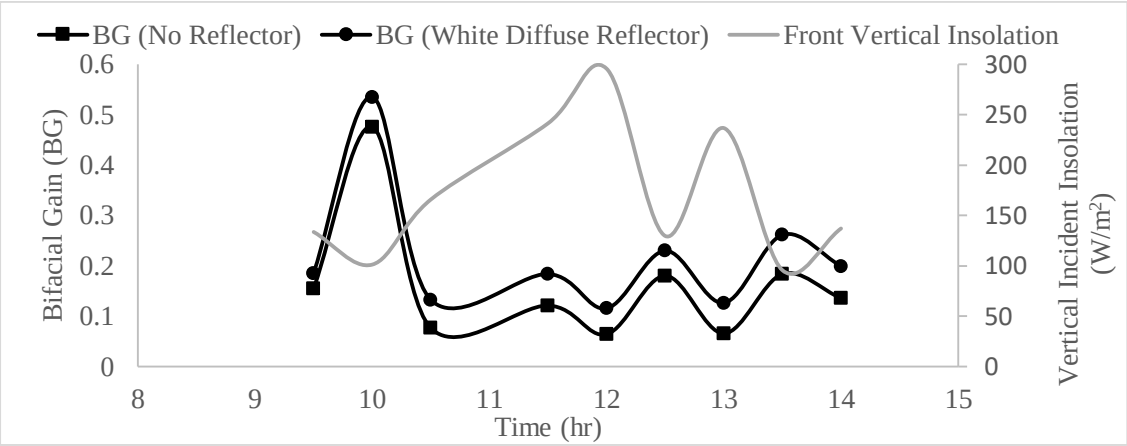

Fig. 9: Experimental data for side by side vertical modules simulating bifacial with no reflector and one enhanced with white diffuse compared to a monofacial panel on July 15, 2021

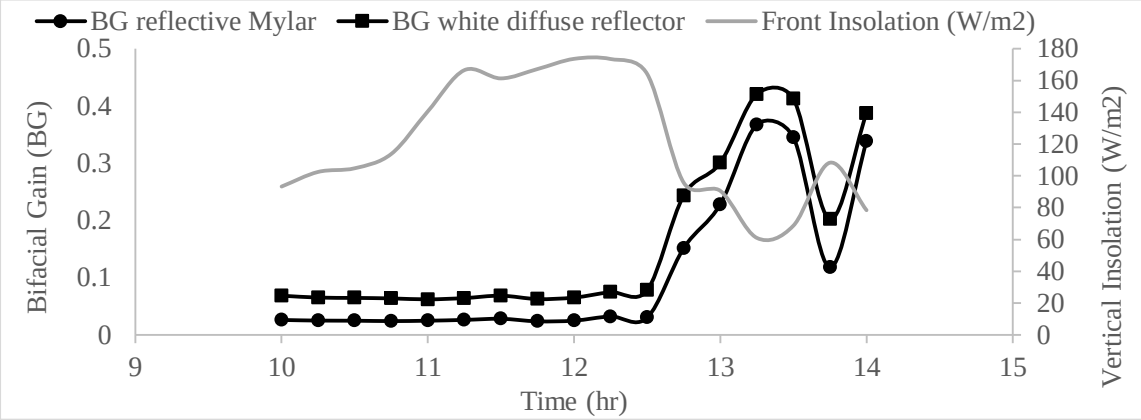

Fig. 10: Experimental data for side by side vertical modules simulating bifacial panels enhanced with a Mylar white diffuse reflectors compared to a monofacial panel on July 9, 2021.

In Figure 10, frames with Mylar and white diffuse reflectors are compared against each other and against a monofacial module. Over the hours tested, the Mylar averaged a BG of 0.11. and the white diffuse averaged 0.16. Overall, from both tests, the white diffuse system yielded about 19% more power than the monofacial module. This could make bifacial panels suitable for roof-tops with white flat or shingle roofs.

5. Conclusions

A model was developed to predict the incident irradiance on the front and rear surface of a bifacial collector equipped with a rear reflector. The model is versatile and can be applied to different locations and for different geometries. It is continuously being improved to capture more and more complex geometry while staying user friendly. Its biggest value may be in defining favorable mounting geometry and configurations in which added reflectors can be complementary to existing ground albedo. The model as it currently stands, only calculates incident irradiance on surfaces. Additional functionality will be needed like module efficiency and temperature dependence to predict the power generated and inform an economic analysis. Experiments were also conducted in this study to provide data to compare to the model and to study the effects of different reflecting surfaces on the bifacial gain. A white diffuse reflector enhanced the bifacial gain over that of the case with no reflector and increased the bifacial gain slightly more than a reflective Mylar film. Bifacial gain is sensitive to time of day and year and to the available beam and diffuse insolation, so its use for informing design must be taken in context. For example, in the summer, due to the large solar altitude angles, reflectors would have to be close to the rear of the collector to capture and reflect beam irradiance, but this could block ground reflectance. In the winter, low solar altitude angles could allow the reflector to be set farther back, not interfering with ground reflected, and reflecting the beam component to the rear of the bifacial module.

6. References

Appelbaum, J., 2016. Bifacial photovoltaic panels field. Renewable Energy. 85, 338-343.

Bergman, T. L., Lavine, A. S., Incropera, F. P., Dewitt, D. P., 2011. Introduction to Heat Transfer 6th Edition, John Wiley and Sons, NJ.

Cuevas, A., Luque, A., Eguren, J., Del Alamo, J., 1982. 50 Per Cent More Output Power from an Albedo-Collecting Flat Panel Using Bifacial Solar Cells. Solar Energy, 29, 419-420.

Duffie, J.A., Beckman, W.A. , 2013. Solar Engineering of Thermal Processes, 4th. edition, Wiley, Hoboken, NJ.

Durusoy, B., Ozden, T, Akinoglu, B. G., 2020. Solar irradiation on the rear surface of bifacial solar modules: a modeling approach. Scientific Reports 10, 13300.

Guerrero-Lemus, R., Vega, R., Kim, T., Kimm, A., and Shephard, L.E., 2016. Bifacial solar photovoltaics – A technology review. Renewable and Sustainable Energy Reviews, 60, 1533-1549.

Hansen, C. W., Stein, J. S., Deline, C., MacAlpine, S., Marion, B., Asgharzadeh, A., Toor, F., 2016. Analysis of Irradiance Models of Bifacial PV Modules. IEEE, 978-1-5090-2724-8/16,138-143.

Jäger, K., Tillmann, P., and Becker, C., 2020. Detailed illumination model for bifacial solar cells. Optics Express, 28, 4751-4762.

Guo, S., Walsh, T.M., Peters, M., 2013. Vertically mounted bifacial photovoltaic modules: A global Analysis. Energy. 61, 447-454.

Jakobsen, M.L., Thorsteinsson, S. Poulsen, P.B., Rodder, P.M., Rodder, K., 2016. Vertical reflector for bifacial PV-panels. Proceedings of the 43rd IEEE Photovoltaic Specialist Conference, 2678-2681.

Joge, T., Eguchi, Y., Imazu, I., Araki, I., Uematsu, T., Matsukuma, K., 2002. Applications and Field Tests of Bifacial Solar Modules. Proceedings of the 29th IEEE Photovoltaic Specialists Conference, 1549-1552.

Khan, M.R., Hanna, A., Sun, X., Alam, M.A., 2017. Vertical bifacial solar farms: Physics, design, and global optimization. Applied Energy. 206, 240-248.

Karahara, N., Yoshioka, K., Saitoh, T., 2003. Performance Evaluation of Bifacial Photovoltaic Modules for Urban Application. 3rd World Conference on Photovoltaic Energy Conversion, 2455-2458.

Kreinin, L., Bordin, N., Karsenty, A., Drori, A., Grobgeld, D., Eisenberg, N., 2010. PV Module Power Gain Due to Bifacial Design, Preliminary Experimental and Simulation Data. IEEE, 978-1-4244-5892-9/10, pp. 2171-2175.

Lim, Y. S., Lo, C. K., Kee, S. Y., Ewe, H. T., Faidz, A. R., 2013. Design and evaluation of passive concentrator and reflector systems for bifacial solar panel on a highly cloudy region – A case study for Malaysia. Renewable Energy, 63, 415-425.

Moehlecke, A., Febras, F.S., Zanesco, I., 2013. Electrical performance analysis of PV modules with bifacial silicon solar cells and white diffuse reflector. Solar Energy. 96, 253-262.

NSRDB: National Solar Radiation Database, last modified 2020, accessed July 29, 2020, nsrdb.nrel.gov

Pelaez, S.A., Deline, C, MacAlpine, S.M., Marion, B.,Stein, J.S., Kostuk, R.K., Comparison of Bifacial Solar Irradiance Model Predictions With Field Validation. 2019. IEEE J. of Photovoltaics. 9, 82-88.

Ooshaksaraei, P., Sopian, K. Zulkifli, R., Alghoul, M.A., Zaidi, S.H.. 2013. Characterization of Bifacial Photovoltaic Panel Integrated with External Diffuse and Semimirror Type Reflectors. Intl. J. of Photoenergy. 2013, 465837.

Sun, X., Khan, M. R., Deline, C., Alam, M. A., 2017. Optimization and performance of bifacial solar modules: A global perspective. Applied Energy. 212, 1601-1610.

Yusufoglu,U.A. Lee, T.H., Pletzer, T.M., Halm, A., Koduvelikulathu, L.J., Comparotto, C., Kopecek, R. Kurz, H., 2014. Simulation of energy production by bifacial modules with revision of ground reflection. Energy Procedia 55, 385-395.

Yusufoglu,U.A.. Pletzer, T.M., Halm, A., Koduvelikulathu, L.J., Comparotto, C., Kopecek, R. Kurz, H., 2015. Analysis of the Annual Performance of Bifacial Modules and Optimization Methods. IEEE J. of Photovoltaics. 5, 320-328.